Reinforced Elastic Layered Systems

CONSTANTINE A. VOKAS AND ROBERT D. STOLL

A continuum model is used to describe the response of a horizontally layered elastic system containing one or more reinforcing sheets that may be located at any prescribed depth below the surface. The analysis is based on well-known equations for layered systems from the linear theory of elasticity. The effect of reinforcing is included by specifying the interlayer boundary conditions on the basis of an analysis that is similar to that used in the classical theory of thin plates. Numerical results are presented for the case of an axisymmetric load applied at the surface of a two-layered system with different combinations of elastic moduli and reinforcing stiffness. The results of these computations represent a limiting case that should be approached by more general models when nonlinear and inelastic effects are made small. Moreover, in many cases in which normal working loads are expected, the analysis will provide a good approximation for the trends that result from various changes in thickness and stiffness of the components.

For the last two decades the practice of reinforcing soil with tension-resistant materials has been widely implemented in geotechnical engineering. Even though examples of using reinforcing materials for strengthening soil foundations date back to the Roman Empire, it was not until Henri Vidal, a French architect and engineer, in the late 1950s, investigated the effects of reinforcement in soil with the aim of improving its mechanical properties that a new era in earth construction began. Reinforcement can take many forms, depending on the material used. Common forms are metallic sheets and meshes, bars, metallic or glass fiber strips, polymer grids, and high-modulus fabrics. The advent of new, stronger, and nondegradable synthetic textile materials and the development of modern synthetic polymer chemicals such as polyamides and polyesters, along with the ever-accelerating development of technical expertise, have led to new, more economical applications in civil engineering practice. Typical applications include construction of railroads, temporary and permanent roads, parking lots, storage-handling sites, and other facilities over poor subgrades; building of facilities of almost any nature over permafrost, muskeg, and other soils in cold weather regions; and construction of earth dams and embankments over compressible fine-grained or peat soils.

A considerable amount of research on reinforced soil systems has been undertaken by numerous universities and research establishments throughout the world over the last two decades, and there is an ever-increasing number of experimental investigations that have demonstrated the efficacy of tension-resistant inclusions in improving the response of reinforced soil systems. However, considering the widespread use of such systems, only a limited amount of theoretical work that describes the detailed mechanisms of the reinforced earth systems has been published. Moreover, many of these investigations are based on limit state theories or simple mechanical models that do not permit a complete description of the stress and displacement field of the system.

Three different approaches have been used to solve the problem of reinforced layered systems. The first is modeling of such systems by simple mechanical models. The distribution of stresses on top of the inclusion is computed by using either the Boussinesq solution for a semi-infinite halfspace *(1, 2)*, a probabilistic concept for the stress diffusion in particulate media *(3)*, or other approximate geometrical methods *(4–6)*. The inclusion is modeled as an elastic or viscoelastic material described mathematically either by a differential equation appropriate for a membrane or an equation derived from an assumed geometry of the deflected and stretched inclusion. The subgrade is represented either by a series of springs or by elastoplastic models, in which an elastic analysis based on a coefficient of subgrade reaction is coupled with a rigid-plastic analysis. Tensile stresses in the inclusion, vertical displacements on top of the subgrade, and other quantities are then computed by applying the equilibrium equations in the vertical and horizontal directions.

In a somewhat different approach, some authors have used continuum models to simulate the effects of horizontal reinforcement. Harrison and Gerrard *(7)* considered a series of equally spaced sheets occurring either in one, two, or three orthogonal sets and applied a theory defining an equivalent homogeneous material that can represent a sequence of alternating orthorhombic layers. Barvashov et al. *(8)* used an elastic solution for a layered system reinforced with a membrane but did not satisfy the equation of equilibrium for the inclusion in the vertical direction.

The third approach involves the use of the finite element method, employed with a varying degree of sophistication in modeling the soil layers and the inclusion at the interface. Examples of this approach include the work done by Barksdale et al. *(9)*, Al-Hussaini and Johnson *(10)*, Raad *(11)*, Andrawes et al. *(12)*, Chang and Forsyth *(13)*, Rowe *(14)*, and Salomone et al. *(15)*. Romstad et al. *(16)*, Shen et al. *(17)*, Herrmann and Al-Yassin *(18)*, and Naylor *(19)* combined the finite element method and the composite stress concept to model the properties of an orthorhombic material that is equivalent to a nonlinear soil reinforced by a set of thin strips.

The finite element approach is a powerful method and, depending on the degree of sophistication, is capable of describing almost any kind of reinforced layered system. Various kinds of inelastic behavior and nonlinearity can be incorporated into a finite element analysis, provided that a realistic set of constitutive equations can be defined for the soil and reinforc-

Department of Civil Engineering and Engineering Mechanics, Columbia University, New York, N.Y. 10027.

ing material. In addition, discontinuities in the displacement field (i.e., slip at the interfaces) and finite strains can also be accommodated. Nevertheless, certain problems require special care in the use of this powerful tool. The necessity of using a finite domain in the calculations and the heavy computational effort required can both lead to unrealistic results unless great care is exercised. Moreover, improperly posed constitutive equations can lead to instabilities, particularly when loading and unloading are not precisely defined. For these reasons it is always good practice to test a program for various limiting cases for which the analytical solution is known. Thus many solutions from the theory of elasticity have played an important role in the development and verification of different finite element codes in many areas of solid mechanics.

In this paper a continuum model that represents a horizontally layered system containing one or more reinforcing sheets located at any prescribed depths below the surface is described. The objective is to define a linear model that closely matches the geometry of real horizontally layered systems containing only a few discrete reinforcing sheets, as opposed to the many closely spaced sheets assumed in some prior investigations *(7)*. Moreover, discontinuities will be allowed both in the normal and tangential tractions across any of the discrete reinforcing sheets because this assumption is more realistic than the membrane analogy used in some previous work *(8)*. Both axisymmetric and plane strain loading on the surface of the layered system have been considered, and stresses and displacements have been calculated for a variety of different combinations of reinforcing stiffness, soil layer thickness, and relative rigidity of the soil layers. Because no interlayer slippage or nonlinearity of material properties is included, the solutions represent a limiting case that should be approached by more general models when the nonlinear and inelastic effects are made small. Furthermore, in cases for which stresses are the result of normal working loads so that inelastic effects are small, the results of the linear analysis should produce a good approximation to the trends that result from various changes in the thickness and stiffness of the different components.

THEORETICAL FORMULATION

Engineers have made extensive use of the theory of elasticity for the calculation of stresses and displacements in soil media. Among the most notable examples is Burmister's solution for layered systems *(20)*. His work has been used for many years as a basis for determining stresses and displacements in highway pavements. Although problems in the theory of elasticity are restricted to consideration of ideal materials and ideal boundary conditions, they have been found to be of practical use in studies of imperfectly elastic and somewhat nonhomogeneous materials, such as soils. The extent to which the computed results approximate the actual response of the system depends on how closely the conditions of the problem can be linearized in the analysis. The authors make no claim that such an approach is the best for estimating inclusion properties for final design, but they do believe that it is advantageous to have a theoretical yardstick to compare with other mathematical or empirical methods.

The system to be analyzed and the cylindrical coordinate system (r, θ, z) that is used are shown in Figures 1 and 2, respectively. The system may have an arbitrary number of horizontal layers, of which the lowermost one is considered to be of infinite extent in both the horizontal and vertical directions. The thickness of the individual layers and the physical properties of the material may vary from one layer to the next, but in any one layer the material is assumed to be homogeneous, isotropic, and linearly elastic. The modulus of elasticity and Poisson's ratio of the jth layer are E_j and ν_j, respectively. The depth to the jth interface is H_j. Any number of thin, linearly elastic, horizontal reinforcing inclusions may be introduced in the system, either at the interface of two adjacent layers or at any depth within a soil layer. The elastic constants of the inclusion are E_g and ν_g and its thickness is t_g. In the case in which an inclusion is introduced within a soil layer and not

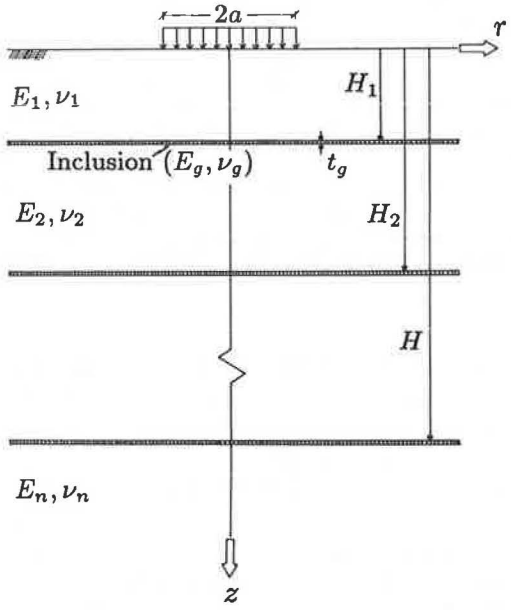

FIGURE 1 Reinforced layered elastic system.

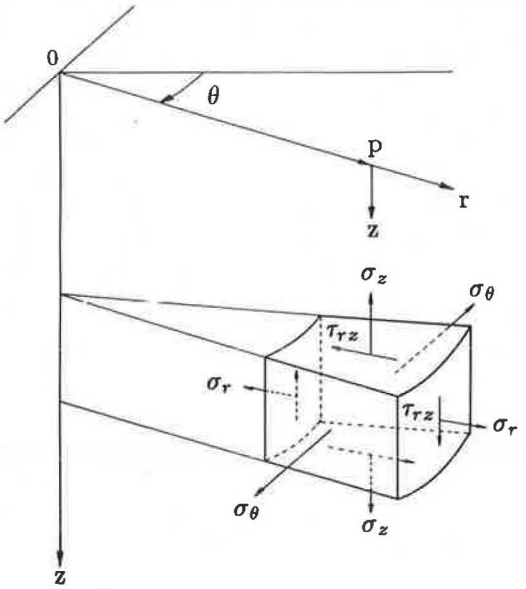

FIGURE 2 Axisymmetric coordinate system.

at an interface, the layer is subdivided into two distinct layers that have the same elastic constants, and the inclusion is introduced at their newly formed interface. It is assumed that there is no slippage between either surface of an inclusion and the adjacent soil strata. The method of analysis that is adopted is based on the classic solution of multilayer elastic systems *(20, 21)* but differs in the way the boundary conditions are handled to take into account the reinforcing action of the inclusions.

As in prior work on layered systems, a stress function ϕ_j that satisfies the governing differential equation

$$\nabla^4 \phi_j = 0 \tag{1}$$

is assumed for each of the layers. For systems with an axially symmetrical stress distribution

$$\nabla^4 = \left(\frac{\partial^2}{\partial r^2} + \frac{1}{r}\frac{\partial}{\partial r} + \frac{\partial^2}{\partial z^2} \right) \left(\frac{\partial^2}{\partial r^2} + \frac{1}{r}\frac{\partial}{\partial r} + \frac{\partial^2}{\partial z^2} \right) \tag{2}$$

in which r and z are the cylindrical coordinates in the radial and vertical directions, respectively. After the stress function is found, the stresses and displacements for each layer can be determined from the following equations:

$$(\sigma_r)_j = \frac{\partial}{\partial z}\left(\nu_j \nabla^2 \phi_j - \frac{\partial^2 \phi_j}{\partial r^2} \right) \tag{3a}$$

$$(\sigma_\theta)_j = \frac{\partial}{\partial z}\left(\nu_j \nabla^2 \phi_j - \frac{1}{r}\frac{\partial \phi_j}{\partial r} \right) \tag{3b}$$

$$(\sigma_z)_j = \frac{\partial}{\partial z}\left[(2 - \nu_j)\nabla^2 \phi_j - \frac{\partial^2 \phi_j}{\partial z^2} \right] \tag{3c}$$

$$(\tau_{rz})_j = \frac{\partial}{\partial r}\left[(1 - \nu_j)\nabla^2 \phi_j - \frac{\partial^2 \phi_j}{\partial z^2} \right] \tag{3d}$$

$$(u)_j = -\frac{1 + \nu_j}{E_j} \frac{\partial^2 \phi_j}{\partial r \partial z} \tag{3e}$$

$$(w)_j = \frac{1 + \nu_j}{E_j}\left[2(1 - \nu_j)\nabla^2 \phi_j - \frac{\partial^2 \phi_j}{\partial z^2} \right] \tag{3f}$$

where $(\sigma_z)_j$, $(\sigma_r)_j$, and $(\sigma_\theta)_j$ are the normal stresses, $(\tau_{rz})_j$ is the shear stress, and $(u)_j$ and $(w)_j$ are the displacements in the radial and vertical directions for the jth layer.

Because Equation 1 is a fourth-order differential equation, the determination of stresses and displacements requires four constants of integration that must be determined from the boundary and interface conditions. Let $\rho = r/H$ and $\zeta = z/H$ be the dimensionless cylindrical coordinates, in which H is the distance from the surface to the upper boundary of the lowest layer. Consider a layered system subjected to a normal pressure $p_m^*(\rho)$ and a horizontal shearing traction $\tau_m^*(\rho)$, to be referred to as basic loads, identified by asterisk superscripts and defined by the equations

$$p_m^*(\rho) = -p_m J_0(m\rho) \tag{4a}$$

and

$$\tau_m^*(\rho) = \tau_m J_1(m\rho) \tag{4b}$$

where p_m and τ_m are the maximum intensities of the applied load. J_0 is the Bessel function of the first kind of order zero and J_1 is the Bessel function of the first kind of order one; m is a continuous parameter that arises when a Hankel transform is used in the solution of Equation 1. The basis loads will be summed to approximate any prescribed distribution of axisymmetric surface tractions.

It can be easily verified by substitution that

$$\phi_j = \frac{H^3}{m^3 p_m}\left[A_{mj} e^{-m(\zeta_j - \zeta)} - B_{mj} e^{-m(\zeta - \zeta_{j-1})} + C_{mj}\, m\zeta e^{-m(\zeta_j - \zeta)} - D_{mj} m\zeta e^{-m(\zeta - \zeta_{j-1})} \right] J_0(m\rho) \tag{5}$$

is a stress function for the jth layer, which satisfies Equation 1; A_{mj}, B_{mj}, C_{mj}, and D_{mj} are the integration constants; and the subscript j refers to the quantities corresponding to the jth layer and varies from 1 to n. By substituting Equation 5 into Equations 3, expressions for the stress and displacement components for each layer can then be obtained.

As mentioned previously, four integration constants need to be evaluated for the determination of stresses and displacements for each layer. For a system composed of n layers, the $4n$ unknowns are obtained from the conditions at the boundaries and interfaces. They depend on the parameter m, the relative stiffnesses of both layers and inclusion, the Poisson's ratios of the materials involved, and the geometry of the system.

If the n-layer system bounded by the surface $\zeta = 0$ is loaded by a vertical stress p_m^* and a tangential traction τ_m^*, then the first two boundary conditions, which describe the surface loading, are

$$(\sigma_z^*)_1 = p_m^* \tag{6a}$$

and

$$(\tau_{rz}^*)_1 = \tau_m^* \tag{6b}$$

in which the asterisk indicates that these quantities correspond to the effect of the basic loads defined by Equations 4.

Two more boundary conditions result from the requirement that the displacements and stresses must vanish at infinite depth. It can be shown that the two integration constants for the lowermost layer ($j = n$) are

$$A_{mn} = C_{mn} = 0 \tag{7}$$

The situation at the $n - 1$ interfaces between the n layers gives rise to the remaining $4(n - 1)$ boundary conditions. It is assumed that there is continuous contact and no slip occurs between layers and inclusions. By denoting the radial and vertical displacements of the inclusion by $\hat{u}$ and $\hat{w}$, respectively, and neglecting all displacement gradients across the small thickness of the much stiffer inclusion, one obtains

$$(u^*)_j = (u^*)_{j+1} = \hat{u}^* \tag{8a}$$

and

$$(w^*)_j = (w^*)_{j+1} = \hat{w}^* \tag{8b}$$

at $\zeta = \zeta_j$, where ζ_j is the depth to the jth interface. This simplifying assumption greatly reduces the amount of computational effort required, while still allowing for different normal traction components on the top and bottom of the reinforcement.

The use of the equilibrium equations for the inclusion gives rise to the two last conditions. By applying the equilibrium equation in the radial direction and assuming plane stress conditions for the inclusion, the following expression is obtained:

$$\frac{d\hat{F}_r}{d\rho} + \frac{\hat{F}_r - \hat{F}_\theta}{\rho} = (\tau^*_{rz})_j - (\tau^*_{rz})_{j+1} \tag{9}$$

where $\hat{F}_r$ and $\hat{F}_\theta$ are the forces per unit length of section within the inclusion. When Hooke's law and the strain-displacement equations for the inclusion are used, expressions for the forces in the radial and tangential directions can be derived in terms of the vertical and radial displacements at the bottom of the upper layer ($\zeta = \zeta_j$). Equation 9 then becomes:

$$\frac{E_g \delta_g}{(1-\nu_g^2)} \left[\frac{d^2(u^*)_j}{d\rho^2} + \frac{d(u^*)_j}{\rho d\rho} - \frac{(u^*)_j}{\rho^2} \right] = (\tau^*_{rz})_j - (\tau^*_{rz})_{j+1} \tag{10}$$

in which the asterisk again identifies the effects due to the basic load; $\delta_g = t_g/H$ is the inclusion's dimensionless thickness. Similarly, by considering equilibrium in the vertical direction and assuming small displacements, one obtains the following equations:

$$\frac{d\hat{F}_{rz}}{d\rho} + \frac{\hat{F}_{rz}}{\rho} = (\sigma^*_z)_j - (\sigma^*_z)_{j+1} \tag{11}$$

The transverse shear force $\hat{F}_{rz}$ that is due to the flexing of the inclusion is derived by considering equilibrium of moments about the circumferential direction:

$$\frac{d\hat{M}_r}{d\rho} + \frac{\hat{M}_r - \hat{M}_\theta}{\rho} = \hat{F}_{rz} \tag{12}$$

By substituting the moment curvature equations in Equation 12, an expression for $\hat{F}_{rz}$ in terms of the displacements can be obtained. Then Equation 11 becomes

$$\frac{E_g \delta_g^3}{12(1-\nu_g^2)} \left[\frac{d^4(w^*)_j}{d\rho^4} + \frac{2}{\rho} \frac{d^3(w^*)_j}{d\rho^3} - \frac{1}{\rho^2} \frac{d^2(w^*)_j}{d\rho^2} + \frac{1}{\rho^3} \frac{d(w^*)_j}{d\rho} \right] = (\sigma^*_z)_j - (\sigma^*_z)_{j+1} \tag{13}$$

Equations 10 and 13, which are similar to the ones used in thin plate theory (22), are the two last expressions needed for the determination of the integration constants for each layer. It can be easily verified that in the case for which no tension-resistant inclusion exists at the interface, the two conditions for the rough interface result from the previous equations by setting $\delta_g = 0$. Substitution of the expressions for the stress and displacement components obtained previously into the boundary and interface conditions yields expressions for the $4n - 2$ unknown integration constants needed for the determination of the stress and displacement components for each layer.

To find the stresses and displacements due to a prescribed axisymmetric vertical or tangential load, p or τ, respectively, one uses a Hankel transform. These loads may be expressed in the form

$$p(\rho) = \int_0^\infty p_m J_0(m\rho)\, dm \tag{14a}$$

and

$$\tau(\rho) = \int_0^\infty \tau_m J_1(m\rho)\, dm \tag{14b}$$

where,

$$p_m = m \int_0^\infty p(s) s J_0(ms)\, ds \tag{15a}$$

and

$$\tau_m = m \int_0^\infty \tau(s) s J_1(ms)\, ds \tag{15b}$$

The integrals in Equations 15a and 15b are the Hankel transforms of the functions $p(\rho)$ and $\tau(\rho)$. The subscript m in p_m and τ_m denotes their dependence in the continuous parameter m of the Hankel transform. Recalling Equations 4, Equations 14 may also be written

$$p(\rho) = \int_0^\infty p^*_m(\rho)\, dm \tag{16a}$$

and

$$\tau(\rho) = \int_0^\infty \tau^*_m(\rho)\, dm \tag{16b}$$

As shown in Equations 16, the desired loading function is expressed as a linear combination of an infinity of other functions that have desirable mathematical properties. Accordingly, after denoting by S^*_m and U^*_m the generalized quantities that describe the effect on the stress and displacement components due to the basic loading p^*_m or τ^*_m, respectively, the effects S and U produced by the actual load p or τ are then expressed

$$S(\rho, \zeta) = \int_0^\infty S^*_m(\rho, \zeta)\, dm \tag{17a}$$

$$U(\rho, \zeta) = \int_0^\infty U^*_m(\rho, \zeta)\, dm \tag{17b}$$

NUMERICAL CALCULATION

The parameters affecting the behavior of the reinforced layered system are the moduli of elasticity and the Poisson's ratios of the layers and the inclusion, their respective thicknesses, and the geometrical distribution of the surface loading. In the analysis, the quantities describing the geometry of the problem are made dimensionless by dividing them by an arbitrary distance, taken here as the distance between the free surface and the upper boundary of the lowermost layer, H. The moduli of elasticity of the soil layers enter as a dimensionless ratio describing the relative rigidity of two adjacent layers. Another dimensionless factor, λ_G, is used in the presentation of results. This factor describes the relative stiffness of the inclusion with respect to the lowermost soil layer and is given by

$$\lambda_G = \frac{E_g t_g}{E_n H} \tag{18}$$

The determination of the stress and displacement components S and U, respectively, produced by the prescribed load at the surface, involves the numerical evaluation of the integrals given by Equations 17. To evaluate these integrals, one must determine the integration constants A_{mj}, B_{mj}, C_{mj}, and D_{mj}, which are functions of the Hankel transform parameter m. A Gaussian quadrature scheme of variable order (from 4 to 256) has been used for this purpose, with the order depending on the degree of accuracy desired. The domain of integration was divided into a finite number of intervals, bounded by the subsequent zeros of one of the two Bessel functions involved. The number of intervals depends on the rate of convergence of the integration. The integration constants were evaluated by solving the $4n - 2$ simultaneous equations obtained from the boundary conditions. To calculate a stress or displacement component at a point, one solves these equations $s \times N$ times, s being the point number of the Gaussian quadrature formula and N being the number of intervals. For a two-layer system, the numerical integration was greatly accelerated by one refinement. The six integration constants required for the complete description of the stress and displacement components were obtained in the form of explicit expressions by using MACSYMA, a symbolic manipulator program. The complete expressions obtained for the cases of either a normal or horizontal traction at the surface may be found in the literature *(23)*.

RESULTS AND CONCLUSION

Figures 3–5 show the effect of a reinforcing inclusion inserted at the interface of a two-layer system. Because of space restrictions and the large number of parameters involved, it is possible to present only a few typical cases to illustrate the response of the reinforced system. In the examples shown, a two-layer system is loaded by a uniformly distributed normal load p_0 covering a circular area of dimensionless radius α, equal to

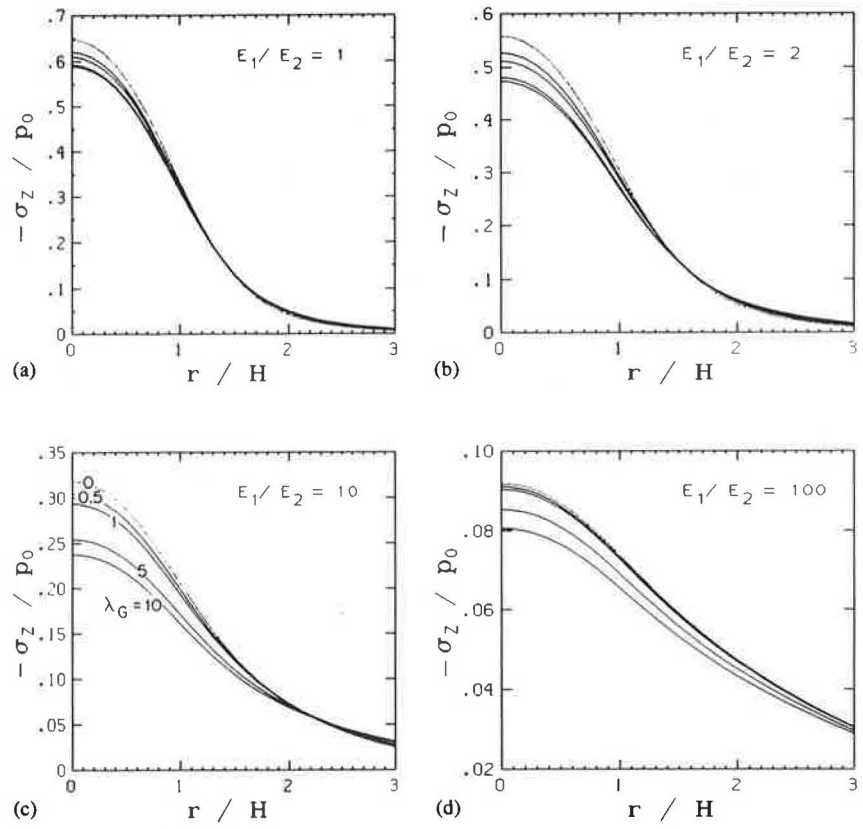

FIGURE 3 Vertical stress distribution on top of the subgrade for a reinforced two-layer system with varying reinforcement stiffnesses λ_G and different soil layer elastic modulus ratios E_1/E_2. $\alpha = 1$, $\nu_1 = \nu_2 = \nu_g = 0.25$. The curves corresponding to different values of λ_G in Figures 3a, 3b, and 3d follow the same order as in Figure 3c.

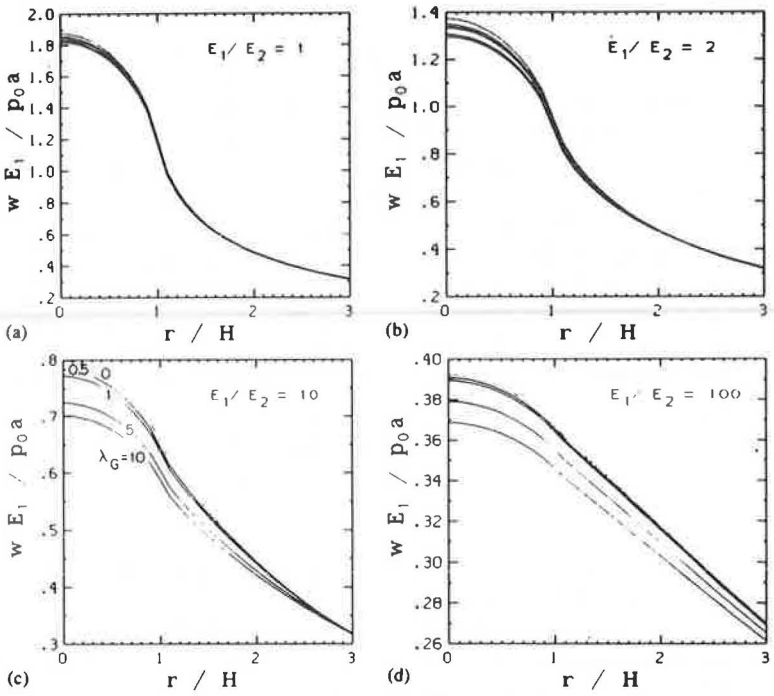

FIGURE 4 Vertical displacement at the free surface for a reinforced two-layer system with varying reinforcement stiffnesses λ_G and different soil layer elastic modulus ratios E_1/E_2. $\alpha = 1$, $\nu_1 = \nu_2 = \nu_g = 0.25$. The curves corresponding to different values of λ_G in Figures 4a, 4b, and 4d follow the same order as in Figure 4c.

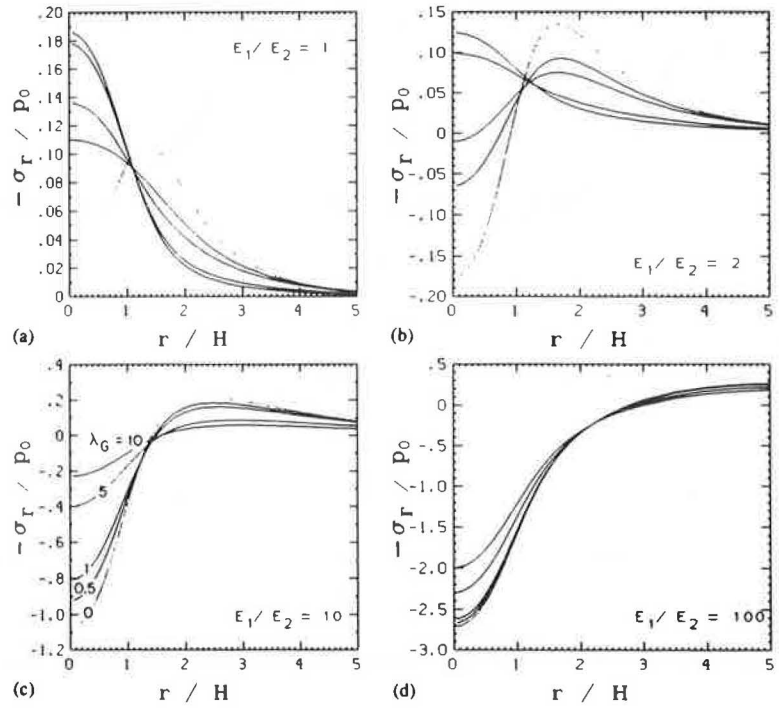

FIGURE 5 Radial stress distribution at the bottom of the top layer for a reinforced two-layer system with varying reinforcement stiffnesses λ_G and different soil layer elastic modulus ratios E_1/E_2. $\alpha = 1$, $\nu_1 = \nu_2 = \nu_g = 0.25$. The curves corresponding to different values of λ_G in Figures 5a, 5b, and 5d follow the same order as in Figure 5c.

the actual radius of the loaded area a divided by H, the distance between the free surface and the interface. In these examples the thickness of the upper layer is equal to the radius of the loaded area, and δ_g is taken equal to 0.01, 0.005, 0.001, and 0.0005. The Poisson ratios of the top and bottom layer and the inclusion are all taken equal to 0.25. Results are plotted for four different values of the ratio E_1/E_2 and for four values of λ_G, the relative stiffness of the inclusion given by Equation 18.

In Figures 3a–3d, the vertical stress on top of the lower layer is plotted as a function of distance away from the axis of symmetry and compared to the stress in an unreinforced ($\lambda_G = 0$) two-layer system. In all cases there is a decrease in the stress, especially out to a distance of about one radius from the axis of symmetry. The vertical displacements at the free surface are shown in Figures 4a–4d for the same combination of parameters. These figures show a favorable but relatively small decrease in settlement beneath the loaded area. A third set of figures (Figures 5a–5d) shows the radial stress at the bottom of the upper layer for the same two-layer system. The tendency for layered systems to develop tensile stresses in this region has always been a problem, and this set of figures shows the beneficial effect of reinforcing in alleviating this problem.

It is concluded that calculations based on the linear theory of elasticity can provide many insights into the effects produced by reinforcing of the type that is incorporated into layered systems, such as those used in pavement and railroad foundations. By using modern high-speed computers and an efficient computational scheme, one can economically study and compare many different cases. Moreover, the results of these computations represent an important limiting case for more involved and expensive calculations that attempt to include nonlinear effects and more detailed material models.

REFERENCES

1. J. D. Nieuwenhuis. Membranes and the Bearing Capacity of Roadbases. *Colloque International sur l'Emploi des Textiles en Geotechnique*, Vol. 1, Paris, April 1978, pp. 3–8.
2. J. B. Sellmeijer, C. J. Kenter, and C. Van Der Berg. Calculation Method for a Fabric Reinforced Road. In *Proc., 2nd International Conference on Geotextiles*, Vol. 2, 1982, pp. 393–398.
3. P. L. Bourdeau, M. L. Harr, and R. D. Holtz. Soil-Fabric Interaction—An Analytical Model. In *Proc., 2nd International Conference on Geotextiles*, Vol. 1, 1982, pp. 387–392.
4. J. P. Gourc, Y. Matichard, H. Perrier, and P. Delmas. Bearing Capacity of a Sand-Soft Subgrade System with Geotextile. In *Proc., 2nd International Conference on Geotextiles*, Vol. 2, 1982, pp. 411–416.
5. J. P. Giroud and L. Noiray. Design of Geotextile Reinforced Unpaved Roads. *Journal of the Geotechnical Engineering Division*, ASCE, Vol. 107, No. GT9, Sept. 1981, pp. 1233–1254.
6. V. D. Kasarnovsky, A. G. Polunovsky, and B. P. Brantman. Design of a Temporary Road Structure with the Use of a Textile Membrane. In *Proc., 2nd International Conference on Geotextiles*, Vol. 2, 1982, pp. 371–374.
7. W. J. Harrison and C. M. Gerrard. Elastic Theory Applied to Reinforced Earth. *Journal of the Geotechnical Engineering Division*, ASCE, Vol. 98, No. SM12, Dec. 1972, pp. 1325–1345.
8. V. A. Barvashov. Analysis of Stresses and Strains in Multi-Layered Soil Foundation Reinforced with Synthetic Fabrics. *Colloque International sur l'Emploi des Textiles en Geotechnique*, Vol. 1, Paris, April 1978, pp. 95–98.
9. R. Barksdale, Q. Robnett, J. Lai, and A. Zeevaert-Wolff. Experimental and Theoretical Behavior of Geotextile Reinforced Aggregate Soil Systems. In *Proc., 2nd International Conference on Geotextiles*, Vol. 2, 1982, pp. 375–380.
10. M. M. Al-Hussaini and L. D. Johnson. Numerical Analysis of Reinforced Earth Wall. *Symposium on Reinforced Earth*, ASCE Annual Convention, Pittsburgh, Pa., April 1978.
11. L. Raad. Reinforcement of Transportation Support Systems through Fabric Prestressing. In *Transportation Research Record 755*, TRB, National Research Council, Washington, D.C., 1980, pp. 49–51.
12. K. Z. Andrawes, A. McGown, R. F. Wilson-Fahmy, and M. M. Mashhour. The Finite Element Method of Analysis Applied to Soil-Geotextile Systems. In *Proc., 2nd International Conference on Geotextiles*, Vol. 3, 1982, pp. 695–700.
13. J. C. Chang and R. A. Forsyth. Finite Element Analysis on Reinforced Earth Wall. *Journal of the Geotechnical Engineering Division*, ASCE, Vol. 103, No. GT7, July 1977, pp. 711–724.
14. R. K. Rowe. Reinforced Embankments: Analysis and Design. *Journal of the Geotechnical Engineering Division*, ASCE, Vol. 110, No. GT2, Feb. 1977, pp. 231–246.
15. W. G. Salomone, R. D. Holtz, and W. D. Kovacs. A New Soil-Reinforcement Interaction Model. *Symposium on Reinforced Earth*, ASCE Annual Convention, Pittsburgh, Pa., April 1978.
16. K. W. Romstad, L. R. Herrmann, and C.-K. Shen. Integrated Study of Reinforced Earth. I: Theoretical Formulation. *Journal of the Geotechnical Engineering Division*, ASCE, Vol. 102, No. GT5, May 1976, pp. 457–471.
17. C.-K. Shen, K. M. Romstad, and L. R. Herrmann. Integrated Study of Reinforced Earth. II: Behavior and Design. *Journal of the Geotechnical Engineering Division*, ASCE, Vol. 102, No. GT6, June 1976, pp. 577–590.
18. L. R. Herrmann and Z. Al-Yassin. Numerical Analysis of Reinforced Soil Systems. In *Proc., Symposium on Reinforced Earth*, ASCE Annual Convention, Pittsburgh, Pa., April 1978.
19. D. J. Naylor. A Study of Reinforced Earth Wall Allowing Strip Slip. *Symposium on Reinforced Earth*, ASCE Annual Convention, Pittsburgh, Pa., April 1978.
20. D. M. Burmister. The General Theory of Stresses and Displacements in Layered Soil Systems. *Journal of Applied Physics*, Vol. 16, 1945, pp. 89–94, 126–127, 296–302.
21. M. R. Mehta and A. S. Veletsos. *Stresses and Displacements in Layered Systems*. Civil Engineering Studies, Structural Research Series, No. 178, University of Illinois, 1959.
22. L. H. Donnell. *Beams, Plates and Shells*. McGraw-Hill, New York, 1976.
23. C. A. Vokas. *Reinforced Layered Elastic Systems*. Ph.D. dissertation, Department of Civil Engineering and Engineering Mechanics, Columbia University, New York, May 1987.

Publication of this paper sponsored by Committee on Mechanics of Earth Masses and Layered Systems.